Proceedings of NAMRI/SME, Vol. 40, 2012

Improved Reduced Order Modeling of Machine Tool Structures

Mohit Law, Yusuf Altintas, and A. Srikantha Phani
Department of Mechanical Engineering
The University of British Columbia
2054-6250 Applied Science Lane
Vancouver, B.C. V6T 1Z4, Canada

ABSTRACT

Dynamic response of a machine tool structure varies along the tool path depending on the changes in its structural configurations. The productivity of the machine tool varies as a function of its Frequency Response Function (FRF) which determines its dynamic response and chatter stability. This paper presents a computationally efficient reduced order model to simulate the FRF at the tool centre point of a machine tool for any position within its work volume. The machine tool is represented by its time invariant components or substructures. The substructures are assembled by modeling the contacts at assembly joints. As the machine tool moves, the contact points are updated to predict the FRFs efficiently without having to use the computationally costly full order Finite Element or Modal models. To facilitate dynamic substructuring, improved variants of reduced order models are developed which automate reduced order determination via retaining only the important modes of the subsystems. Position-dependent dynamic behavior and stability is successfully simulated for the case of virtual three axis milling machine, using the developed substructurally synthesized reduced order model.

KEYWORDS

Machine tools, Model reduction, Substructuring, Dynamics

INTRODUCTION

The dynamic stiffness at the tool centre point (TCP) is crucial for the stability of machine tools; stability being characterized in terms of vibrations at the TCP. Lack of sufficient dynamic stiffness may lead to a regenerative chatter vibration which is detrimental to the performance and integrity of entire machine tool system resulting in: poor surface quality; accelerated tool wear; damage of work piece and machine structural elements; and, ultimately limiting productivity [1]. Machine tool stability is governed both by the tool-tool holder-spindle characteristics and by the modal properties, i.e. the eigenfrequencies and mode shapes of the machine tool structural elements. These modal properties in turn are a function of the instantaneous position of machine structural elements within the work volume, caused by relative motion between flexible structures resulting in position (time) varying boundary conditions. Experimental procedures called ‘acceptance tests’ [2] are developed to obtain the position-dependent behavior of machine tools that are already built. Based on these tests, cutting parameters are varied along the tool path to ensure a stable cut, or, more conservatively, cutting parameters are selected based on the absolute minimum stability limit for all positions, which may result in a loss of productivity. Hence, it becomes crucial that the dynamic response be estimated at the design stage, and appropriate design modifications be made, such as to guarantee a target productivity, thereby eliminating the need to build costly and time prohibitive physical prototypes.

State-of-the-art design, development, and analyses of dynamic response of machine tools is based on finite elements (FE) models [3]. FE models have very large order, typically 1,000,000 degrees of freedom (DOFs) or more for a typical three axis machine tool. Dynamic response analyses at discrete positions for such large order models require cumbersome adaptive meshing to account for the position-dependent boundary conditions. Recent trends are to treat this class of problems using co-simulation with FE solvers coupled to standard flexible multibody dynamic analysis software [4, 5]. These co-simulations are time prohibitive, and are restricted to flexible bodies attached at geometrically fixed contact points, hence not suitable for flexible machine tool structural elements undergoing relative motion; which is essentially a case of multiple geometrically changing contact points that change as the tool moves from one position to another.

Previous research related to modeling of systems with position-dependent dynamics has largely centered on: evaluating response at a few discrete positions [6]; or reducing the moving contact problem to that of a rigid body in contact with and moving over a flexible body with uniform nodal spacing [7, 8]. This paper presents position-dependent modeling of flexible bodies in contact at multiple points (nodes), which has not been considered earlier. A general framework is developed in which substructures are coupled at their interfaces using novel adaptations of constraint formulations. Adjacent flexible bodies are synthesized by describing displacement compatibility with sets of algebraic equations, which are updated to account for relative motion. The organization of this paper is summarized in Figure 1.

To facilitate a moving contact model, necessary model reduction of the large order FE models based on improved variants of the standard component mode synthesis (CMS) methods are developed and applied. The reduced models must be of a manageable size, while retaining the dynamic characteristics of the full model. A major challenge with using CMS scheme, is deciding the number of mode sets from the individual components to be retained. Usually, either the first few low frequency modes; or modes with an eigenfrequency up to 1.5-2 times the maximum excitation frequency are retained [9], this however increases the size of the reduced model. An accurate representation of the full frequency spectrum while retaining computationally efficiency requires answering the following question: *how many and which modes of the subsystem need to be retained?*

Modal methods of mode selection [10, 11] based on 'dominance measures' require converting the large scale second order ordinary differential equations obtained from the FE model to a linear first order state-space model, resulting in even larger system matrices. Other methods [9, 12, 13] sort and retain the most significant modes based on the strength of interaction between the subsystem and the main system. Their main concern however, was not the dynamical substructural system, but its effect on the main system. Alternatively, suitable subspace dimension determination may be carried out using an adaptive refinement method as in [14], wherein modes were included/ excluded iteratively from each subspace depending upon how posteriori error estimates of each CMS subspace influenced the error in the synthesized reduced model. Though automated, it is computationally expensive and inefficient.

The present work aims at developing accurate reduced order substructural models whose dynamic characteristics are independent of its position. The important modes identified from the system frequency response function (FRF) simulated between the point(s) are those which possess high degree of controllability and observability. The proposed approach for determining mode cut-off number also automates reduced model order determination.

Generalized modeling of position-dependent dynamics is presented in the next section, followed by improved variants of the CMS schemes. The substructurally synthesized reduced order model (ROM) is applied to a three axis Cartesian milling machine, and effects of position-dependent structural dynamics on the chatter stability of milling operations are discussed, followed by the main conclusions.

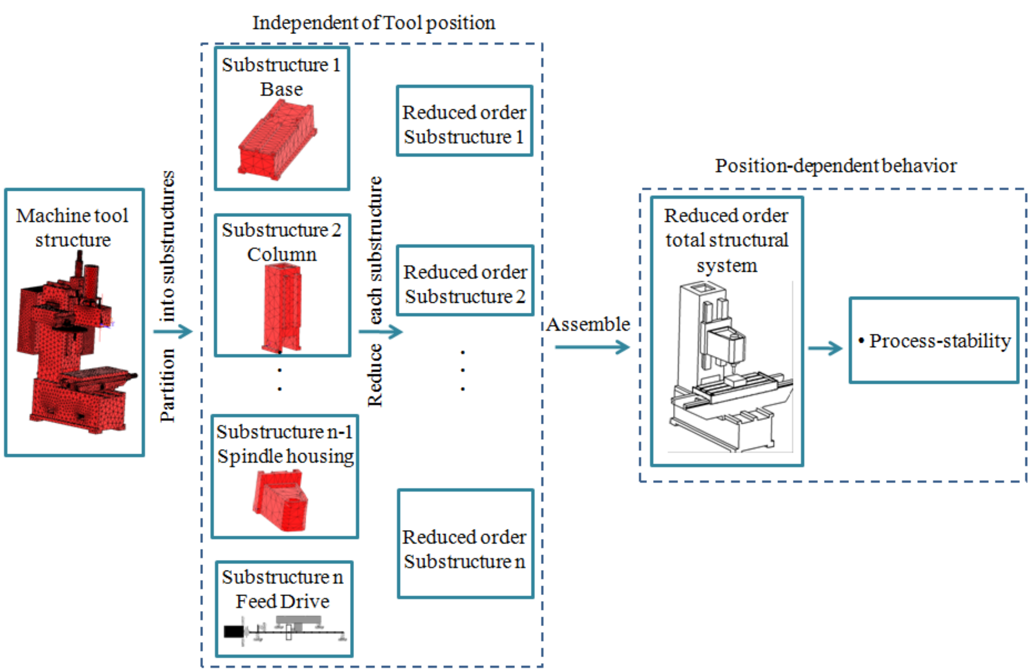

Figure 1. Proposed modeling scheme overview.

GENERALIZED SUBSTRUCTURAL FORMULATION FOR POSITION-DEPENDENCY

Machine tools may be treated as an assembly of flexible multibodies; each a substrucutral component modeled using FE. Main substructural components of a machine tool are: column, bed, table, spindle, and feed drives. The objective of generalized formulation is to predict the dynamic response of the complete machine efficiently as one component changes its position relative to others.

Substructural Compatibility

Consider two substructures $S^{(1)}$ and $S^{(2)}$ as shown in Figure 2; which may represent any of the machine components with relative motion between them. The displacement vector $\boldsymbol{u}^{(n)}$ for substructure n consists of displacements at the interior DOFs $\boldsymbol{u}_{\mathrm{I}}^{(n)}$, and at the exterior DOFs $\boldsymbol{u}_{\mathrm{E}}^{(n)}$. If the substructures are obtained through a partitioning of the FE mesh of the global structure, they are automatically conforming, as in Figure 2(a), for which kinematic interface compatibility conditions require that:

$$\boldsymbol{u}_{\mathrm{E}}^{(1)'} - \boldsymbol{u}_{\mathrm{E}}^{(2)'} = 0 \qquad (1)$$

where $\boldsymbol{u}_{\mathrm{E}}^{(n)'}$ represents a subset of the total DOFs $\boldsymbol{u}_{\mathrm{E}}^{(n)}$ that are in contact at a particular position. This compatibility condition, described by a displacement operator $\boldsymbol{C}^{(n)}$ that extracts the interface DOFs is a Boolean matrix and may be represented as:

$$\boldsymbol{C}^{(n)}\boldsymbol{u}^{(n)} = \begin{bmatrix} \boldsymbol{I}_{\mathrm{E}}^{(n)'} & 0 & 0 \end{bmatrix} \begin{Bmatrix} \boldsymbol{u}_{\mathrm{E}}^{(n)'} \\ \boldsymbol{u}_{\mathrm{E}}^{(n)} - \boldsymbol{u}_{\mathrm{E}}^{(n)'} \\ \boldsymbol{u}_{\mathrm{I}}^{(n)} \end{Bmatrix} \qquad (2)$$

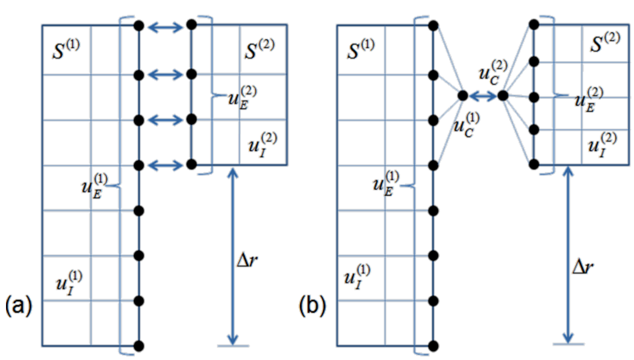

Figure 2. Substructural assembly by enforcing continuity constraints, (a) compatible substructures, (b) incompatible substructures.

If however, the substructures are modeled with different mesh resolutions at interfaces, as in Figure 2(b), the displacement operator $\boldsymbol{C}^{(n)}$ will no longer have the form of a Boolean matrix, and in order to enforce approximate geometric compatibility between substructures, traditionally, Lagrange multipliers are introduced [15]. The Lagrange multipliers approximated by shape functions are not suitable for a position-dependent formulation, since, each time one substructure moves relative to another (say, by changing Δr – Figure 2), a different set of nodes come into contact at the interface, and employing the method in [15] would require a new set of Lagrange multipliers for each new position, which is computationally inefficient.

To synthesize such incompatible meshes, an interpolation multipoint constraint (MPC) equation formulation is employed here. MPCs represent one DOF as a linear combination of other DOFs. The formulation involves defining an artificial condensation node to which the interface nodes are linked using a localized partitioning scheme as shown in Figure 2(b). The kinematic interface compatibility conditions with a condensation node require:

$$\begin{Bmatrix} \boldsymbol{u}_{\mathrm{E}}^{(1)'} \\ \boldsymbol{u}_{\mathrm{E}}^{(2)'} \end{Bmatrix} - \begin{bmatrix} \boldsymbol{C}_{\mathrm{C}}^{(1)} \\ \boldsymbol{C}_{\mathrm{C}}^{(2)} \end{bmatrix} \boldsymbol{u}_C = 0 \qquad (3)$$

which states that the interface displacement along $S^{(1)}$, $\boldsymbol{u}_{\mathrm{E}}^{(1)'}$, must be equal to that of $S^{(2)}$, $\boldsymbol{u}_{\mathrm{E}}^{(2)'}$; $\boldsymbol{C}_{\mathrm{C}}^{(n)}$ is the displacement operator for substructure n, and $\boldsymbol{u}_C$ is the condensation node displacement vector with compatibility of $\boldsymbol{u}_{\mathrm{C}}^{(1)} = \boldsymbol{u}_{\mathrm{C}}^{(2)}$.

Interpolation MPC Formulation

The interface DOFs are linked to the DOFs of the condensation node in the localized partitioning scheme using an interpolation MPC [16]. The formulation presented here, is for the generalized case of an individual substructure, hence the substructure superscript n is dropped. The interpolation MPC formulation defines displacements ($\boldsymbol{u}_C$) and rotations (α_C) of the condensation node as the weighted average of the motion of the interface nodes. The motion of the condensation node is fully described by the displacement of all interface nodes as [16]:

$$\begin{aligned} \boldsymbol{u}_C &= \frac{\sum_{k=1}^{n} w_{\mathrm{E}_k} \boldsymbol{u}_{\mathrm{E}_k}}{\sum_{k=1}^{n} w_{E_k}} \\ \alpha_C &= \frac{\sum_{k=1}^{n} w_{\mathrm{E}_k} \boldsymbol{r}_{Ck} \times \boldsymbol{u}_{\mathrm{E}_k}}{\sum_{k=1}^{n} w_{\mathrm{E}_k} |\boldsymbol{r}_{Ck}|^2} \end{aligned} \qquad (4)$$

where $\boldsymbol{r}_{Ck}$ is the vector from the condensation node to the node corresponding to the interface node k. To insure that the condensation node represents the average motion of the interface, the weight factors w_{E_k} for each DOF should be chosen proportional to the part of the interface surface its node represents, and may be assigned as the coordinates of those nodes. In order for the condensation node to represent the motion of the interface surface, the condensation node should be placed at the center of the interface surface [16]. An interpolation MPC formulation introduces as many additional constraints as there are condensation DOFs.

Numerical Methods to Handle Constraint Equations

On account of constraining the displacements at the interface, the potential energy (PE) of the system is modified by adding an extra "energy" term. The updated potential functional is solved by the Penalty method. The variation of the modified potential functional in its standard form yields [17]:

$$[\boldsymbol{K} + \boldsymbol{C}^T \alpha \boldsymbol{C}]\boldsymbol{u} = \boldsymbol{f} \quad (5)$$

where $\boldsymbol{C}^T\alpha\boldsymbol{C}$ is the penalty matrix; wherein $\boldsymbol{C}$ is the displacement operator; $\alpha = diag[\alpha_1 \quad \alpha_2 \cdots \quad \alpha_m]$ is a diagonal matrix of m penalty numbers corresponding to the m constraint equations; $\boldsymbol{K}$ is the stiffness matrix; and $\boldsymbol{f}$ is the external force vector. If $\alpha = 0$ in Eq. (5), the system of equations returns to the case of no constraints being imposed. As α_i becomes very large, the penalty of violating constraints becomes large, so the constraints are closely satisfied. Numerical stability for this method is a function of the choice of α_i, which may be selected based on guidelines as in [17].

Substructural Synthesis

The assembled undamped equation of motion ensuring compatibility at the interfaces for the two substructures in Figure 2 is represented as:

$$\begin{bmatrix} \boldsymbol{M}^{(1)} & \boldsymbol{0} \\ \boldsymbol{0} & \boldsymbol{M}^{(2)} \end{bmatrix} \begin{Bmatrix} \ddot{\boldsymbol{u}}^{(1)} \\ \ddot{\boldsymbol{u}}^{(2)} \end{Bmatrix} + \begin{bmatrix} \boldsymbol{K}^{(1)} + \boldsymbol{C}^T\alpha\boldsymbol{C} & \boldsymbol{0} \\ \boldsymbol{0} & \boldsymbol{K}^{(2)} + \boldsymbol{C}^T\alpha\boldsymbol{C} \end{bmatrix} \begin{Bmatrix} \boldsymbol{u}^{(1)} \\ \boldsymbol{u}^{(2)} \end{Bmatrix} = \begin{Bmatrix} \boldsymbol{f}^{(1)} \\ \boldsymbol{f}^{(2)} \end{Bmatrix} \quad (6)$$

where $\{\boldsymbol{M}, \boldsymbol{K}\}$ are the substructural mass and stiffness matrices; and $\boldsymbol{C}(\boldsymbol{u}^{(1)}, \boldsymbol{u}^{(2)})$ is the displacement operator coupling the substructures. Employing the floating frame of reference technique, the eigenvalue problem (EVP) in Eq. (6) may be solved for any desired position, by varying the position of the substructure 2, set by Δr (Figure 2), thus obtaining the dynamic response at any position. The selection of appropriate nodes at the interface of the two substructures, and of the weighting coefficients for the generation of the MPC equation set with the compatibility requirement is implemented in the MATLAB environment.

The proposed formulation presents a complete description of modeling the position-dependent dynamics based on defining constraint equations to ensure compatibility of heterogeneous substructures.

MODEL ORDER REDUCTION

Consider the equation of motion in Eq. (6) for the case of undamped FE substructures, at the substructural level:

$$\boldsymbol{M}\ddot{\boldsymbol{u}} + \boldsymbol{K}\boldsymbol{u} = \boldsymbol{f} \quad (7)$$

where $\{\boldsymbol{M}, \boldsymbol{K}\} \in R^{n\times n}$, and $\boldsymbol{f} \in R^{n\times 1}$. The general concept of model order reduction in structural mechanics is to find a low order subspace $\boldsymbol{T} \in R^{n\times m}, m \ll n$, to approximate the displacement vector in Eq. (2) such that:

$$\begin{Bmatrix} \boldsymbol{u}_E \\ \boldsymbol{u}_I \end{Bmatrix} = \boldsymbol{T} \begin{Bmatrix} \boldsymbol{u}_E \\ \boldsymbol{q}_I \end{Bmatrix} \quad (8)$$

where $\boldsymbol{T}$ is the transformation matrix for reduction; and the subscript E and I represent the exterior and interior DOFs respectively. The substrucutral assembly formulation in Eq. (6) may be treated as a generic CMS, for which $\boldsymbol{T}$ is [18]:

$$\boldsymbol{T}_{CMS} = \begin{bmatrix} \boldsymbol{I}_{EE} & \boldsymbol{0}_{EP} \\ \boldsymbol{T}_{S_{IE}} & \boldsymbol{\Phi}_{IP} \end{bmatrix} \quad (9)$$

where $\boldsymbol{I} \in R^{E\times E}$ is a unit matrix; $\boldsymbol{T}_{S_{IE}} = -\boldsymbol{K}_{II}{}^{-1}\boldsymbol{K}_{IE}$; is the equivalent static transformation, and, $\boldsymbol{\Phi}_{IP} \subseteq \boldsymbol{\Phi}_{II}$, obtained by traditionally retaining the first few P modes of the mode shape vector $\boldsymbol{\Phi}_{II}$ is obtained by solving the EVP corresponding to the interior DOFs. To overcome the part static nature of this transformation in Eq. (9), advantageous characteristics of another model order reduction scheme, the so-called iterated 'improved reduction system' (IRSi) method based on [19] are included.

Mode Selection Criteria

To obtain position-independent substructural reduced models which are a function of the selected mode sets of the components in the improved CMS schemes, mode sets are selected as detailed in the flowchart in Figure 3.

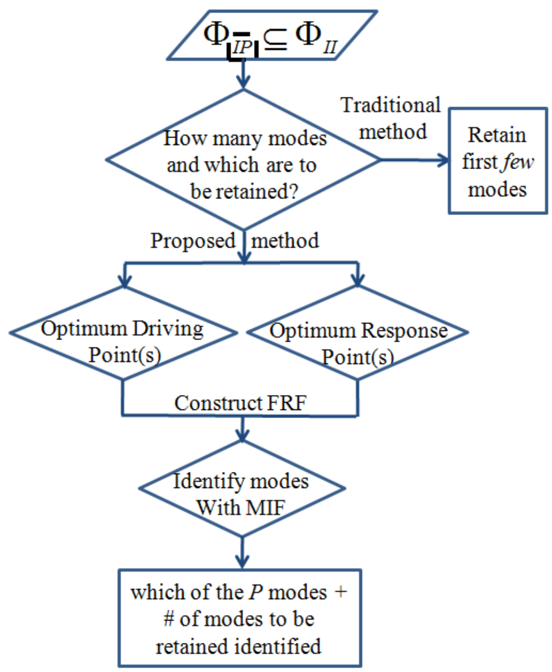

Figure 3. Flow chart for mode selection criterion.

Significant modes are those identified with a mode indicator function (MIF) from a simulated FRF between the locations of highest controllability and observability. To determine the optimal excitation location, the 'optimum driving point(s) (ODP)' method proposed in [20] is employed since it offers a very 'natural' selection criterion based on the computed eigenvectors ($\mathbf{\Phi}_{II}$). Point(s) with large mode shape amplitudes for the modes of interest are selected while avoiding the nodal points or any points near the nodal line. To determine the response location(s), point(s) with the maximum kinetic energy (KE) are chosen. A FRF is simulated between these locations, and a MIF is employed to identify the modes in this FRF. The modes thus identified are treated as significant and are the ones to be retained within the transformation matrix. This improved ROM is referred to as the ICMSi - MIF method in the subsequent sections. The equation of motion in Eq. (6), is transformed using the improved form of Eq. (9) to yield a substructurally sysnthesied reduced order model, which is applied to a three axis milling machine in the next section.

APPLICATION: MODELING A THREE AXIS MILLING MACHINE

The position-dependency of the dynamic stiffness at the TCP of a machine tool is primarily due to the relative motion of the spindle-spindle housing moving over the vertical column. Hence, as a first step only these three substructures (spindle, spindle housing, and column) are considered as ones to be modeled; reduced independently; and combined subsequently using constraint formulations. A special FE spindle model [21] which consists of the spindle shaft and the spindle cartridge – both modeled with Timoshenko's beam elements, along with angular contact ball bearings and other accessories is integrated as a separate substructure coupled rigidly to the spindle housing. The assembled model is assumed to be rigidly connected to the machine base. All other structural elements (base, cross-slide, etc.), and machine accessories are ignored.

FE models for substructures were generated from their respective detailed CAD models. Ten noded solid tetrahedron elements were employed. After necessary convergence tests of FE models, the structural system matrices were exported to the MATLAB environment. All subsequent model order reduction and model synthesis were conducted within the MATLAB environment.

Model Order Reduction (MOR) for Substructures

Reduction was carried out at the substructural level by retaining only the interface (exterior) DOFs. For each substructure two types of interfaces were defined: fixed; and, moving, see Table 1 for division of DOFs by interface type. Moving interfaces involve geometrically changing contacting nodes as one substructure moves over another, while fixed interfaces on the other hand - as the name suggests, are fixed.

Table 1. Division of DOFs by interface type for the substructural components.

		Column	Spindle-Spindle Housing
Full Order Model		10908	15117
ROM	Fixed Interface	312	-
	Moving Interface	762	1845
ROM Total		1074	1845

The interface DOFs were complemented by component generalized coordinates corresponding to the component normal modes identified using the MIF based sorting approach. The FRF was simulated between DOFs of highest controllability and observability up to 10 kHz, while assuming uniform damping for all modes of the level of $\zeta = 0.02$. In this way, 31 significant modes were identified for the spindle-spindle housing (SP-SH) substructure, and 43 for the column (COL) substructure. Table 2 compares modes of the column substructure for reduced order model using the MIF based sorting scheme with that of the standard CMS-Craig and Bampton [18] modal reduction (SMR) scheme, i.e. in which the first few P non rigid-body low frequency modes are retained.

While only the top 10 modes are listed in Table 2, it is evident that the mode sets are disjoint, and, that the MIF based ranking scheme spans a wider frequency range than the SMR based scheme. In the case of the column substructure, for the SMR scheme to span the same frequency range as that of the MIF based scheme, 310 mode sets would need to be retained, instead of the 43 presently identified as significant, thus increasing the size of the reduced model considerably. Moreover, the number of modes identified also serves to decide the order of the reduced model automatically.

Table 2. Top 10 mode subsets for SMR and MIF based sorting for the Column Substructure.

SMR	Mode #	1	2	3	4	5	6	7	8	9	10
	Freq. x 1E+3 [Hz]	0.21	0.48	0.60	0.68	0.86	0.92	0.93	0.96	1.02	1.14
MIF	Mode #	1	4	5	7	9	11	12	13	14	16
	Freq. x 1E+3 [Hz]	0.21	0.68	0.86	0.93	1.02	1.17	1.21	1.33	1.37	1.47

Substructural Assembly for Different Positions of Substructures

Consider the case of the spindle-spindle housing combination in rigid contact with and moving over the column guideways as shown in Figure 4. The substructures, after reduction were synthesized with the interpolation multipoint constraint formulations of Eq. (4). Each condensation node was assumed to have four DOFs, three translational, and, one rotational DOF. The Penalty method was employed to solve the coupled reduced EVP problem of the assembled substructures for a given position using a modified (reduced) form of Eq. (6).

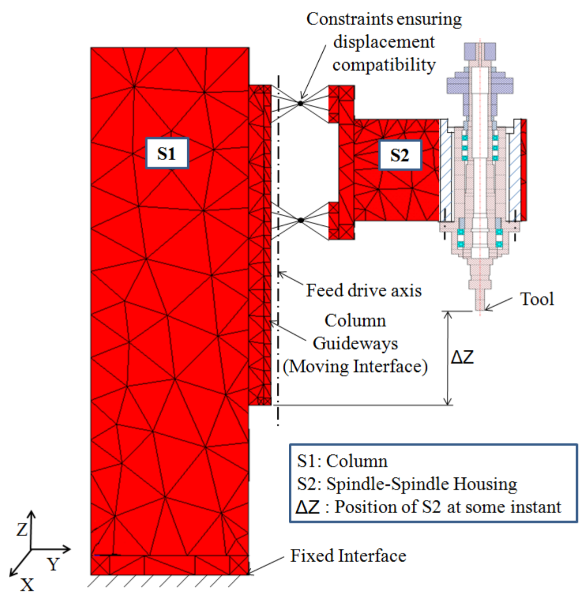

Figure 4. Substructural assembly of the spindle-spindle housing substructure with the column substructure.

To evaluate this reduced order substructurally synthesized position-dependent model, direct TCP FRFs for the ICMSi - MIF variant of the ROM were compared with that of a full order model obtained from ANSYS at three different positions, results of which are shown in Figure 5. The top position is the configuration shown in Figure 4; the mid position; and, the bottom position are when the spindle-spindle housing combine has moved in the negative Z-direction by an amount of 0.2 m; and 0.4 m respectively. A new set of constraint equations are established at each position to describe the relations between the new nodes that have come into contact. Subsequently, the new reduced EVP is solved to obtain the position-dependent response.

The strong position-dependent mode shift and amplitude change in the global modes (corresponding to the column, the spindle housing and the spindle assembly) up to 800 Hz is captured entirely by the substructurally synthesized reduced order models, and, this at a fraction of the computational cost required as compared to full order models. Simulation times are reduced from tens of hours for each position using the full models to less than a minute using the improved reduced models, thereby facilitating further position-dependent stability analysis.

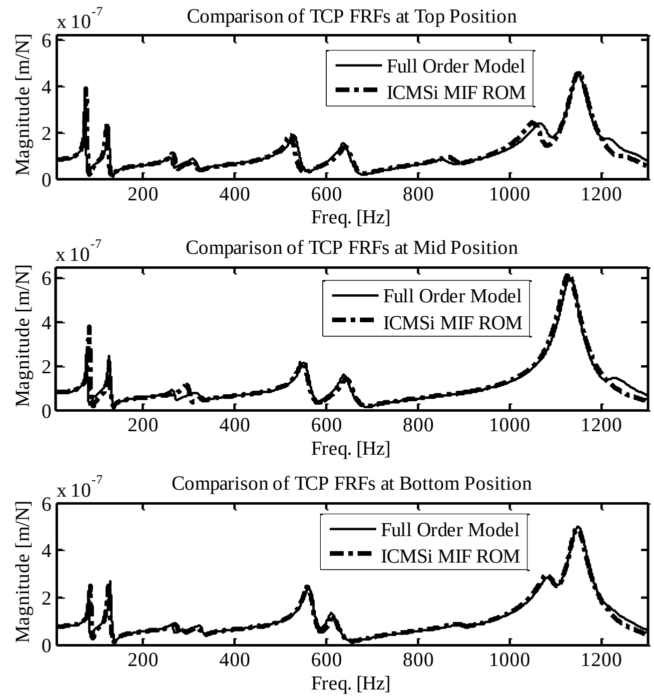

Figure 5. Comparison of ROM and full order model TCP FRFs at three different positions: top position (top), mid position (middle), and bottom position (bottom).

POSITION-DEPENDENT STABILITY

During machining, the frequency content of the force signal may excite one or more of the structural modes of the machine tool. This excitation may lead to a regenerative chatter mechanism, which among other factors, is strongly influenced by the modal parameters of the machine tool. Moreover, because the machine model can now be efficiently reconfigured and assembled in any desired position, this model is utilized to characterize the effects of process machine interactions by way of predicting the position-dependent stability.

The position-dependent stability is evaluated based on a mechanistic model of the milling process [1], and a modal model of the machine to capture the dynamic chip variations due to vibrations. With the single frequency approach for the solution of the stability problem, the characteristic equation of the milling system is given as:

$$det\left([\boldsymbol{I}] - \frac{1}{4\pi}N_t K_t a\left(1 - e^{-i\omega_c T}\right)[\boldsymbol{\alpha}_0][\boldsymbol{\Phi}(i\omega_c)]\right) = 0 \quad (10)$$

where N_t are the number of teeth on the cutter; K_t is the cutting force coefficient of the material being cut; a is the axial depth of cut, ω_c is the chatter frequency; T is the tooth passing period; and α_0 is the matrix of the average direction factors. Φ is the transfer function matrix at the TCP, and may be represented as:

$$[\boldsymbol{\Phi}(i\omega)] = \begin{bmatrix} \Phi_{xx}(i\omega) & \Phi_{xy}(i\omega) \\ \Phi_{yx}(i\omega) & \Phi_{yy}(i\omega) \end{bmatrix} \tag{11}$$

where $\Phi_{xx}(i\omega)$ and $\Phi_{yy}(i\omega)$ are the direct transfer functions in the x and y directions, and where $\Phi_{xy}(i\omega)$ and $\Phi_{yx}(i\omega)$ are the cross transfer functions. To simulate the position dependent stability, $\boldsymbol{\Phi}(i\omega)$ is updated for every position. The stability boundary, i.e. the limiting depth of cut ($a = a_{lim}$), described by the parameters in Eq. (10) is analytically determined as:

$$a_{lim} = -\frac{2\pi\Lambda_R}{N_t K_t}\left[1 + \left(\frac{\Lambda_I}{\Lambda_R}\right)^2\right] \tag{12}$$

where Λ_R and Λ_I are the real and imaginary eigenvalues from the solution to the EVP in Eq. (10). Position-dependent stability was simulated for machining AISI 1045 steel, with the cutting parameters as listed in Table 3.

Table 3. Cutting parameters

Cutter Type – Dia. 20 mm end mill, 30º helix	
N_t	4
K_t	1904 [MPa]
Immersion	Full [100 %]

Chatter stability lobes and the corresponding chatter frequencies are compared for the substructurally synthesized ICMSi - MIF type ROM with full order model results in Figure 6, for two positions: position 1, i.e. top position and position 2, i.e. bottom position. The regions below the stability curve are stable. For the case of machining common steels such as AISI 1045, it is difficult to excite modes > 1000Hz; the excitation frequency being limited by the recommend cutting speeds for milling of such materials. Thence modes beyond this range are ignored in chatter simulation. As was evident in Figure 5, for this frequency range, the dynamic response at position 2 was stiffer than the response at position 1, which should manifest as the stability boundary for this position (position 2) being higher than that at position 1, which is the observed behavior in Figure 6 (left). The strong shifts in chatter frequencies at spindle speeds of ~1500-2500 RPM, corresponding to the shifts in the global modes of the column and the spindle housing are also evident in Figure 6 (right). The results with ROMs are found to be in good agreement with the full order results, with the exception at spindle speed of ~2000 RPM for position 2; which may partially be attributed to numerical errors.

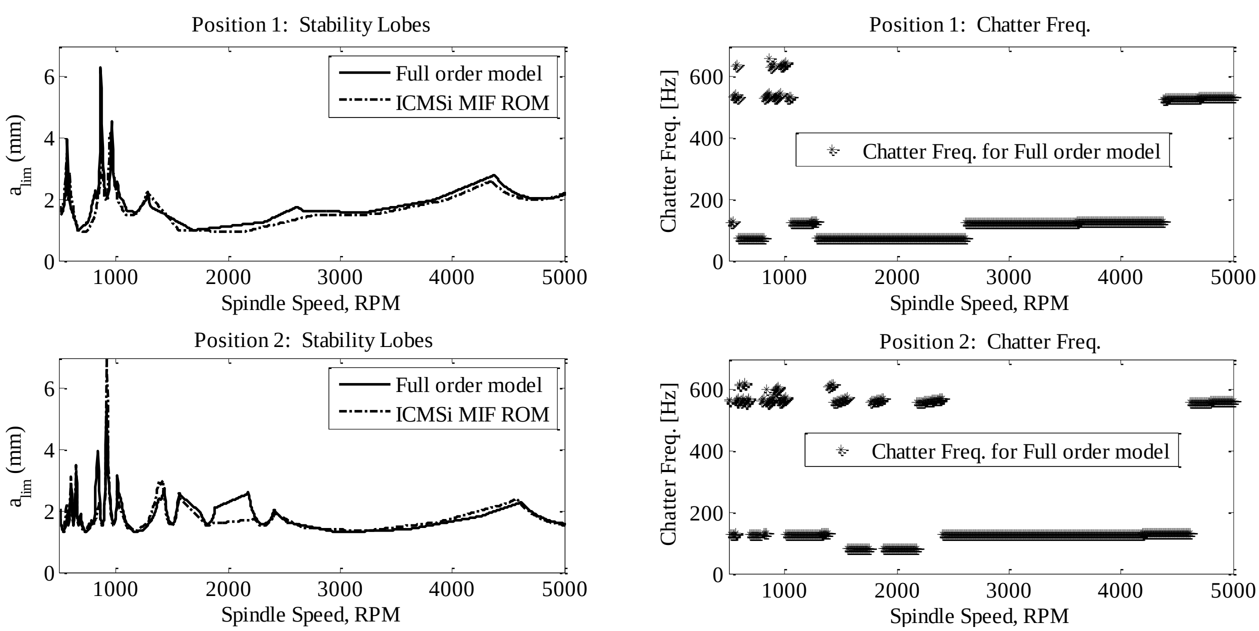

Figure 6. Stability boundaries at two distinct positions (left) and the corresponding chatter frequencies (right) for machining AISI 1045 common steel.

CONCLUSIONS

A systematic procedure is proposed to model and evaluate the position-dependent dynamic behavior of a three axis milling machine tool. Substructurally synthesized reduced order FE models coupled at their interfaces using constraint formulations enable accurate and computationally efficient investigation of the dynamic behavior at any discrete position of the tool within the work volume. Simulation times were reduced from hours for each position using the full models to minutes using the improved reduced models. The ICMSi - MIF ROM with the interpolation MPC formulation was found to approximate the full order response quite well; thus verifying also the accuracy of the improved ROM. Position-dependent stability behavior was efficiently simulated for a given set of cutting conditions.

The MIF based sorting scheme, by virtue of retaining significant modes representing a large frequency spectrum, keeps the order of the reduced model to a minimum.

The substructures were rigidly coupled in this study, without having modeling the stiffness and damping at the joints. This will be part of future research. The ultimate aim of this project is a complete co-simulation of the machine structural dynamics including the feed drive dynamics, the axis position control, the NC interpolation, and the process-machine interactions via a stability model. This synthesized mechatronic machine tool system will allow evaluation and optimization of the dynamic motion performance of the machine tool at the design stage, eliminating the need for costly physical prototyping.

ACKNOWLEDGMENTS

This research has been supported by the NSERC CANRIMT Research Grant.

REFERENCES

[1] Altintas, Y., 2000, Manufacturing Automation: Metal Cutting Mechanics, Machine Tool Vibrations, and CNC Design, Cambridge University Press.

[2] Yigit, A. S., Ulsoy, A. G., 2001, Dynamic Stiffness Evaluation for Reconfigurable Machine Tools Including Weakly Nonlinear Joint Characteristics, IME, Part B: J of Engg. Manufacture, 216: 87-101.

[3] Bianchi, G., et al., 1996, Towards virtual engineering in machine tool design, CIRP Annals 45: 381-384.

[4] Zaeh, M. F., Siedl, D., 2007, A New Method for Simulation of Machining Performance by Integrating Finite Element and Multi-body Simulation for Machine Tools, Annals of the CIRP, 6: 383-386.

[5] Aurich, J. C., et al., 2009, Modelling and simulation of process: machine interaction in grinding, Production Engineering Research and Development, 3: 111-120.

[6] Fonseca, P. D., 2000, Simulation and Optimization of the Dynamic Behavior of Mechatronics Systems, PhD Thesis, Katholieke Universiteit Leuven.

[7] Okwudire, C., 2009, Modeling and Control of High Speed Machine Tool Feed Drives, PhD. Thesis, University of British Columbia.

[8] da Silva, M. M., et al., 2009, Computer-aided integrated design for machines with varying dynamics, Mechanism and Machine Theory 44: 1733-1745.

[9] Givoli, D., et al., 2004, Which are the important modes of a subsystem?, International Journal for Numerical Methods in Engineering 59: 1657-1678.

[10] Litz, L., 1981, Order reduction of linear state-space models via optimal approximation of the non-dominant modes, Large Scale Systems 2: 171-184.

[11] Feliachi, A., 1990, Identification of critical modes in power systems, IEEE Transaction on Power Systems, 5: 783-787.

[12] Shabana, A., Wehage, R., A, 1983, Variable Degree-of-Freedom Component Mode Analysis of Inertia Flexible Mech. Sys., J. of Mechanisms, Transmissions and Automation in Design, 105/371/: 371-378.

[13] Tayeb, S., Givoli, D., 2011, Optimal modal reduction of dynamic subsystems: Extensions and improvements, International Journal for Numerical Methods in Engineering 85: 1-30.

[14] Jakobsson, H., et al., 2011, Adaptive component mode synthesis in linear elasticity, International J. for Numerical Methods in Engineering 86: 829-844.

[15] Farhat, C. G., Geradin, M., 1994, On a component mode synthesis method and its application to incompatible substructures, Computers and Structures 51: 459-473.

[16] Heirman, G., Desmet, W., 2010, Interface reduction of flexible bodies for efficient modeling of body flexibility in multibody dynamics, Multibody System Dynamics 24: 219-234.

[17] Liu, G. R., Quek, S. S., 2003, The Finite Element Method: A Practical Course, Butterworth-Heinemann.

[18] Craig Jr, R. R., and Bampton, M. C. C., 1968, Coupling of substructures for dynamics analyses, AIAA Journal, 6: 1313-1319.

[19] Koutsovasilis, P., Beitelschmidt, M., 2010, Model order reduction of finite element models: improved component mode synthesis, Mathematical and Computer Modelling of Dynamical Sys., 16: 57-73.

[20] Imamovic, N., 1998, Validation of Large Structural Dynamics Models using Modal Test Data, PhD Thesis, Imperial College of Science, Tech. & Med.

[21] Cao, Y., Altintas, Y., 2004, A general method for the modeling of spindle-bearing systems, Transactions of the ASME, 126: 1089-1104.